Research Article

Corresponding author:
Suat Irmak; Email: sfi5068@psu.edu

Evapotranspiration of Palmer amaranth (*Amaranthus palmeri*) in maize, soybean, and fallow under subsurface drip and center-pivot irrigation systems

Jasmine Mausbach[1], Suat Irmak[2], Meetpal S. Kukal[3], Kelsey Karnik[4], Debalin Sarangi[5] and Amit J. Jhala[6]

[1]Graduate Research Assistant, Department of Agronomy and Horticulture, University of Nebraska-Lincoln, Lincoln, NE, USA; [2]Professor and Department Head, Department of Agricultural and Biological Engineering, Penn State University, University Park, PA, USA; [3]Assistant Research Professor, Department of Agricultural and Biological Engineering, Penn State University, University Park, PA, USA; [4]Biomedical Data Scientist, Department of Biostatistics, University of Kentucky, Lexington, KY, USA; [5]Assistant Professor, Department of Agronomy and Plant Genetics, University of Minnesota, St Paul, MN, USA and [6]Associate Professor, Department of Agronomy and Horticulture, University of Nebraska–Lincoln, Lincoln, NE, USA

Abstract

Palmer amaranth (*Amaranthus palmeri* S. Watson) is a major biotic constraint in agronomic cropping systems in the United States. While crop–weed competition models offer a beneficial tool for understanding and predicting crop yield losses, within these models, certain weed biological characteristics and their responses to the environment are unknown. This limits understanding of weed growth in competition with crops under different irrigation methods and how competition for soil moisture affects crop growth parameters. This research measured the effect of center-pivot irrigation (CPI) and subsurface drip irrigation (SDI) on the actual evapotranspiration (ET_a) of *A. palmeri* grown in maize (*Zea mays* L.), soybean [*Glycine max* (L.) Merr.], and fallow subplots. Twelve *A. palmeri* plants were alternately transplanted 1 m apart in the middle two rows of maize, soybean, and fallow subplots under CPI and SDI in 2019 and 2020 in south-central Nebraska. Maize, soybean, and fallow subplots without *A. palmeri* were included for comparison. Soil-moisture sensors were installed at 0-0.30, 0.30-0.60, and 0.60-0.90-m soil depths next to or between three *A. palmeri* and crop plants in each subplot. Soil-moisture data were recorded hourly from the time of *A. palmeri* transplanting to crop harvest. The results indicate differences in *A. palmeri* ET_a between time of season (early, mid-, and late season) and crop type across 2019 and 2020. Although irrigation type did not affect subplot data, the presence of *A. palmeri* had an impact on subplot ET_a across both years, which can be attributed to the variable relationship between volumetric soil water content (VWC) and ET_a throughout the growing season due to advancing phenological stages and management practices. This study provides important and first-established baseline data and information about *A. palmeri* evapotranspiration and its relation to morphological features for future use in mechanistic crop–weed competition models.

Introduction

Palmer amaranth (*Amaranthus palmeri* S. Watson) is the most troublesome weed in agronomic cropping systems in the United States (Heap 2014). Several factors have enabled *A. palmeri* to become such a dominant and difficult-to-control weed, including its rapid growth rate (Ehleringer 1985; Ehleringer and Forseth 1980), prolific seed production (Keeley et al. 1987), and ability to tolerate adverse environmental conditions (Franssen et al. 2001), including disease, genetic abnormalities, and water stress (Chahal et al. 2018). From a 2-yr field study in Kansas, Horak and Loughin (2000) reported that *A. palmeri* had a 50% higher growth rate (i.e., 0.18 to 0.21 cm per growing degree day) and leaf area than redroot pigweed (*Amaranthus retroflexus* L.), tumble pigweed (*Amaranthus albus* L.), and waterhemp [*Amaranthus tuberculatus* (Moq.) Sauer]. In a field trial in Missouri, Sellers et al. (2017) reported a 65% greater dry weight of *A. palmeri* compared with *A. retroflexus* and *A. albus*, *A. tuberculatus*, spiny amaranth (*Amaranthus spinosus* L.), and smooth pigweed (*Amaranthus hybridus* L.) 2 wk after planting. It has also been reported that *A. palmeri* has greater root length and root biomass than most crops, allowing it to occupy a larger soil volume and extract soil nutrients (Wright et al. 1999), leading to crop yield losses if it is not controlled early in the growing season. Annually, weeds cause an estimated economic loss of more than US$100 billion and a 10% yield loss on a global scale (Appleby et al. 2000). In light

of these losses, it is clear that a greater understanding of crop–weed interactions in terms of water, nutrients, light, and competition for other resources is necessary to develop cost-effective and sustainable weed management practices.

Crop–weed competition models offer a significant tool for understanding and predicting crop yield losses due to crop–weed interference. Research is currently dominated by empirical studies in which crop yield loss (or crop yield) and weed threshold values are predicted in response to variable weed density or biomass in certain environmental conditions. Complex empirical models have been developed by considering variables such as multiple weed species in simultaneous competition (Diggle et al. 2003; Firbank and Watkinson 1985; Pantone and Baker 1991; Park et al. 2002), timing of weed emergence (Cousens et al. 1987; Neve et al. 2003), and weeds with multiple emergence patterns (Peltzer et al. 2012). However, within these models, weed biological characteristics are unknown, limiting our understanding of weed growth in competition with crops and how that competition affects crop growth parameters as well as soil water dynamics and water use (evapotranspiration).

At the intersection of weed and crop stomatal behavior, environmental conditions, and soil water availability, evapotranspiration is a major unknown. Crop–weed competition is a complex phenomenon, and for predictive purposes, a detailed mechanistic model offers greater insights than an empirical model. Mechanistic models consider all underlying morphological and physiological processes and their dependence on one another with respect to external forces and time (Singh et al. 2020). However, morphological and physiological plasticity in weed species is a challenge for studies/models that have been developed based on weed growth. Although some research on weed biology and ecology has been conducted, additional systemic studies in different locations and under different environmental conditions are needed to elucidate simulation models and thus weed management decisions (Chauhan and Johnson 2010; Van Acker 2009). Robustly measured evapotranspiration data in systems can aid in strengthening modeling capabilities.

In terms of crop–weed competition, the competitive ability of crops depends on many factors, such as (1) crop type and cultivar or variety selection, sowing date, row spacing, and tillage practice; (2) weed density and composition; (3) soil and climatic factors; and (4) crop rotation (Singh et al. 2020). As the inherent ability of crops to compete against weeds is weakened by climatic and soil stresses (Mohler 2004), the time and method of irrigation management may also impact crop–weed competition, as weeds also benefit from increases in available soil water during irrigation. Additionally, understanding when, where, and how water is consumed by evapotranspiration is useful not only for evapotranspiration analyses, but for improving water use efficiency.

Developing irrigation management strategies based on available soil water requires knowledge of weed and crop responses to water deficits, which can be obtained through modeling (Paredes et al. 2014), relating biomass production to actual evapotranspiration (ET_a). The effects of crop ET_a rates on crop yield are well known; however, there is a lack of scientific information in terms of the effect of weed ET_a on weed morphological features (e.g., biomass, leaf area index, plant height). While empirical crop–weed competition models have been useful, they have not been adequate in predicting crop–weed competition with *A. palmeri* under varying irrigation practices. By adopting a mechanistic approach to examine the effects of irrigation type on *A. palmeri* and crop competition, we can begin to use parameters such as ET_a and total soil water (TSW) to strengthen predictive capabilities of mechanistic crop–weed competition models. Thus, the objective of this research was to determine the effect of center-pivot (CPI) versus subsurface drip irrigation (SDI) systems on the ET_a of *A. palmeri* grown in maize (*Zea mays* L.), soybean [*Glycine max* (L.) Merr.], and fallow systems under the soil, climate, crop, and water management conditions of south-central Nebraska.

Materials and Methods

Plant Materials

Glyphosate-resistant *A. palmeri* seeds were germinated in 11.4-cm-deep square plastic pots in a University of Nebraska–Lincoln greenhouse maintained at 18/24 C day/night temperatures with a 14-h photoperiod. Glyphosate-resistant *A. palmeri* was used so that other weeds could be controlled after *A. palmeri* plants were transplanted in the field. To ensure that *A. palmeri* plants were glyphosate-resistant, glyphosate at 2,526 g ae ha^{-1} mixed with liquid ammonium sulfate at 3% v/v was sprayed on 10- to 12-cm-tall *A. palmeri* plants using an AIXR TeeJet® (TeeJet, Grime, IA) nozzle. The herbicide mixture was applied at a rate of 140.3 L ha^{-1} at 1.0 m s^{-1} using a chamber track sprayer. *Amaranthus palmeri* plants survived the glyphosate application, signifying that the seed source was truly glyphosate resistant.

Field Experimental Design, Site Description, and Crop Management

Field experiments were conducted in 2019 and 2020 growing seasons in the Irmak Research Laboratory's advanced crop production, evapotranspiration, irrigation engineering, plant physiology, and climate change impact on agriculture and water resources research facilities at the University of Nebraska–Lincoln, South Central Agricultural Laboratory near Clay Center, NE (40.57°N, 98.12°W). A large experimental field was divided into CPI and SDI research facilities, both of which irrigation methods were established/installed by the senior author (SI) in 2005. Thus, the field topography, slope, soil characteristics, and other soil- and field-related characteristics of both CPI and SDI fields were similar (Table 1). The CPI field was irrigated using a four-span hydraulic and continuous-move system (T-L Irrigation, Hastings, NE) (Irmak 2015). In the SDI field, 257-m-long drip lines were installed 0.40 m below the soil surface and were centered in the interrow area of every other plant row. Irrigation was applied directly to the crop root zone via drip emitters spaced approximately 0.45 m apart along the drip lines (Netafim-USA, Fresno, CA) (Irmak 2010). Typical effective rooting depth of field maize in the experimental site is 1.2 m. The 30-yr average rainfall in the area during the growing season (May to August) is 112.4 mm, with significant annual and growing season variability in both timing and magnitude (de Sanctis and Jhala 2021; Irmak 2010, 2015). Rainfall data from the 2019 and 2020 growing seasons are presented in Figure 1.

The experiment was carried out as a split-plot design with two levels of irrigation assigned at the whole-plot level: CPI and SDI. At the split-plot level, six crop types were assigned to subplots. Nonrandomized subplots consisted of maize, soybean, and no crop (i.e., fallow) with *A. palmeri*; and maize, soybean, and fallow without *A. palmeri*. Maize, soybean, and fallow subplots without *A. palmeri* were included for TSW and actual evapotranspiration (ET_a) data comparisons with subplots containing *A. palmeri*. Each subplot measured 3-m wide by 9-m long, with four rows of maize or soybean in the subplots containing these crops. The field was rolling stalk-chopped without tillage. A broadcast application of

Table 1. Field and soil characteristics of center-pivot and subsurface drip irrigation fields.

Characteristics	Hastings silt loam soil
	— % —
Slope	0.5 north-south
Sand	15
Clay	20
Silt	65
Organic matter	2.5
	— $m^3\ m^{-3}$ —
Field capacity	0.34
Permanent wilting point	0.14
Saturation	0.53

11-52-0 N-P-K at 168 kg ha^{-1} and an in-furrow injection of 32-0-0 N-P-K at 201 kg ha^{-1} were applied across the entire experimental site before crops were sown. 'Dekalb DKS 60-87RIB' maize was planted at a depth of 5.0 cm and rate of 85,000 seeds ha^{-1}. 'NK S29-K3X' soybean was planted at a depth of 3.8 cm and rate of 375,000 seeds ha^{-1}.

Once *A. palmeri* plants reached a height of 18 to 25 cm in the greenhouse, 12 plants were alternately transplanted 1 m apart in the two center rows of the subplots assigned *A. palmeri*. A premix of saflufenacil–imazethapyr–pyroxasulfone (Zidua® PRO herbicide) (Zidua Pro herbicide, Research Triangle Park, NC) (Acuron herbicide, Greensboro, NC) was applied at 215 g ai ha^{-1} to soybean; a premix of atrazine–bicyclopyrone–mesotrione–*S*-metolachlor (Acuron® herbicide) was applied at 2.4 kg ai ha^{-1} to maize and fallow; and a postemergence application of glyphosate at 1,263 g ha^{-1} was applied across all plots for control of existing weeds.

Measurement of Soil Water Status and Irrigation Management

Watermark Granular Matrix Sensors (Irrometer, Riverside, CA) were installed next to three *A. palmeri* plants or crop plants and between three *A. palmeri* and crop plants in each subplot to measure soil matric potential (SMP) on an hourly basis. The sensors were buried at 0- to 0.30-m, 0.30- to 0.60-m, and 0.60- to 0.90-m soil depths, and hourly data were collected from the *A. palmeri* transplant date to shortly before crop harvest in both years. A total of 45 and 54 sensors were installed across the subplots of each irrigation system in 2019 and 2020, respectively. The sensors were connected to model 900M Watermark Monitor data loggers (Irrometer). SMP measurements were converted to percent volumetric soil water content (VWC) using predetermined soil water retention curves for the same experimental field (Irmak 2019a, 2019b):

$$\theta_v = (3 \times 10^{-6} \times SMP^2) - (0.0013 \times SMP) + 0.3764 \quad [1]$$

where θ_v is the VWC (% vol or $m^3\ m^{-3}$), and SMP is the soil matric potential (kPa). VWC was converted to TSW by adding the VWC values at each sensor depth and multiplying by a conversion value of 3.048 (ft to mm). The TSW in the complete monitored soil profile (0 to 0.90 m) reflects the daily integration of soil moisture detected at individual incremental depths throughout the profile. Sensor data were used to determine crop and *A. palmeri* evapotranspiration using the soil water balance approach and for irrigation timing. Irrigation was initiated under CPI and SDI when the average SMP values of the top 0.90 m were approximately 100 to 110 kPa (Irmak et al. 2012, 2016), which translates to a depletion of soil water in the crop root zone of 40% to 45% below field

capacity (Irmak 2019a, 2019b). This SMP range was implemented to prevent water stress. Irrigation of 32 mm was applied once per experimental field between July 31 and August 2 of 2019. In 2020, irrigation of 32 mm was applied six times per experimental field between July 13 and September 1.

Seasonal Actual Evapotranspiration Using Soil–Water Balance

Crop and *A. palmeri* actual evapotranspiration (ET$_a$, mm) were calculated for each experimental subplot using the procedures outlined in Irmak (2015) by implementing a soil water balance equation:

$$P + I + U + R_{on} = R_{off} + D + \Delta SWS + ET_a \quad [2]$$

where *P* is precipitation (mm), *I* is irrigation water applied (mm), *U* is upward soil-moisture flux (mm), R_{on} is surface run-on within the field (mm), R_{off} is surface runoff from individual treatments (mm), ΔSWS is change in soil water storage in the root zone soil profile (mm), and *D* is deep percolation below the crop root zone (mm). *U* was assumed to be zero, as the groundwater depth in the experimental field is about 33 to 35 m below the surface (Irmak 2010). Deep percolation was estimated by a soil water balance approach using a program written in Microsoft Visual Basic (Bryant et al. 1992; Irmak 2015). Inputs to the program include initial water content of the soil profile at crop emergence, irrigation date and amount, maximum rooting depth, crop maturity date, soil parameters, and daily weather data (i.e., incoming shortwave radiation, relative humidity, air temperature, precipitation, and wind speed). The program calculated daily ET$_a$ and the water balance in the crop root zone using the two-step approach (ET$_a$ = K_c × ET$_0$), where ET$_o$ is evapotranspiration of a grass reference crop, and K_c is the crop coefficient. In the program, ET$_o$ is calculated using weather data as the input to the Penman-Monteith equation (Monteith 1965), and K_c is used to adjust the estimated ET$_o$ for the reference crop to that of the desired crops at different growth stages and environments (Irmak 2015). The daily soil water balance equation used for calculating deep percolation as presented in Irmak (2015) is:

$$D_j = \max\left(P_j - R_j + I_j - ET_{aj} - CD_{j-1}, 0\right) \quad [3]$$

where D_j is deep percolation on day *j* (mm), P_j is precipitation on day *j* (mm), R_j is precipitation and/or irrigation runoff from the soil surface on day *j* (mm), I_j is irrigation depth on day *j* (mm), ET$_{aj}$ is crop or *A. palmeri* actual evapotranspiration on day *j* (mm), and CD_j is root zone cumulative depletion depth at the end of day *j* − 1, estimated using the two-step approach (Irmak 2015). Following Irmak (2015), R_{off} from individual treatments was estimated using the USDA-NRCS curve number method. As suggested by Irmak (2015), according to the silt loam soil at the experimental site and the known land use, slope, and conservation tillage, curve number *C* = 75 was used. Assuming *U* and R_{on} are negligible, the soil water balance equation was reduced to the following form for calculating crop and *A. palmeri* ET$_a$ (Irmak 2015):

$$ET_a = P + I - R_{off} - D \pm \Delta SWS \quad [4]$$

Growth Index, Plant Biomass, and Total Leaf Area Measurements

Three *A. palmeri* plants were selected and sampled at four removal timings according to soybean growth stage. Soybean growth stage was selected instead of maize growth stage, because it was easier to
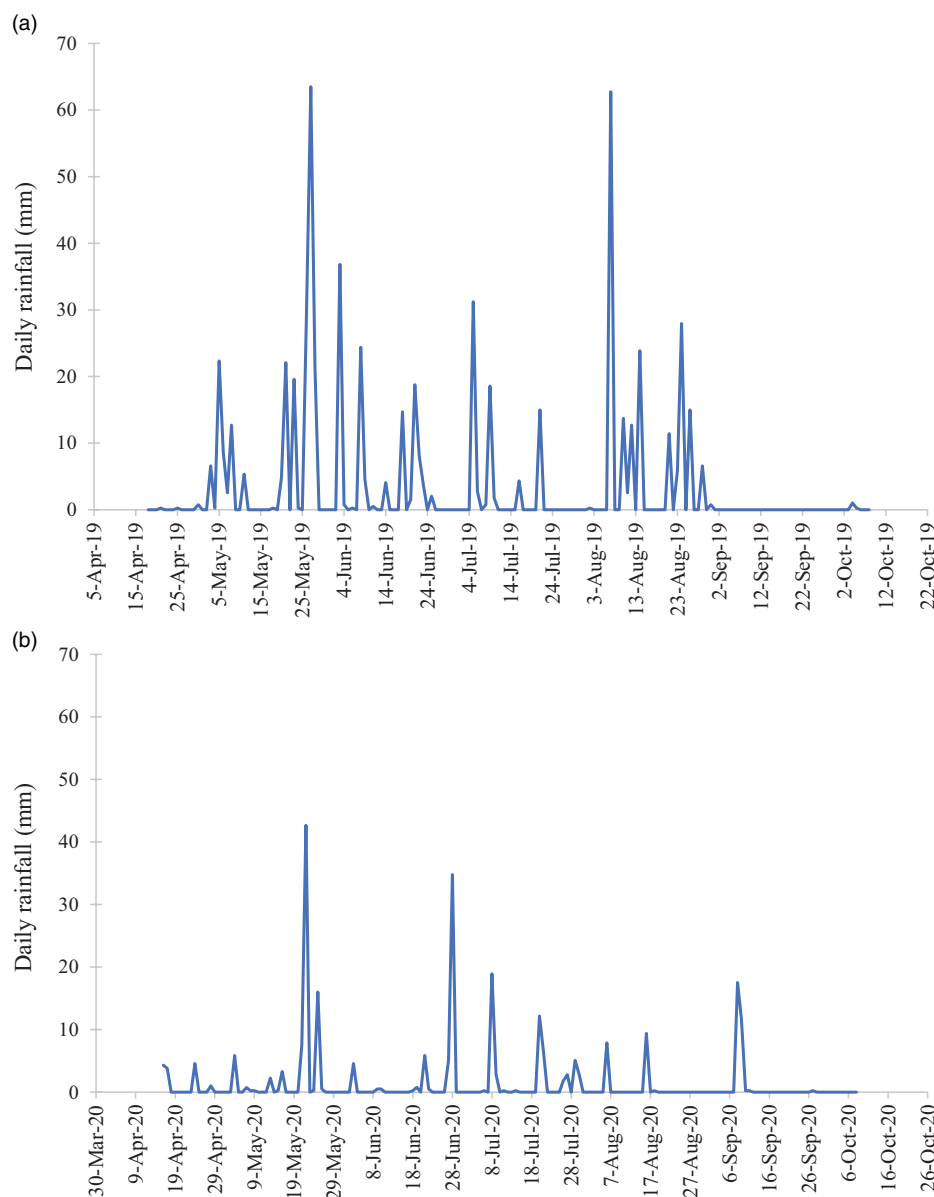
Figure 1. Daily rainfall in (A) 2019 and (B) 2020 growing seasons at the experimental site (University of Nebraska–Lincoln, South Central Agricultural Laboratory near Clay Center, NE).

visually determine compared with maize. Removal timings occurred at V4, R1, R3, and R5 soybean growth stages in 2019, and at R1, R3, R5, and R6 soybean growth stages in 2020. The later removal timings in 2020 were a result of COVID-19 delays. Growth index, plant biomass, and total leaf area of each *A. palmeri* plant were determined at these removal timings and then averaged over all subsampled replicates for a total of 24 sample units each growing season. Growth index was calculated using the following equation (Irmak et al. 2004; Sarangi et al. 2015):

$$GI \ (cm^3) \ = \ \pi \ \times \ (w/2)^2 \ \times \ h \qquad [5]$$

where *w* is the width of the plant calculated as an average of two widths, one measured at the widest point and another at 90° to the first; and *h* is the plant height measured from the soil surface to the shoot apical meristem. After plant height and width measurements were taken, leaves were counted and removed from each *A. palmeri*

plant to measure total leaf area using a leaf area meter (LI-3100C Area Meter, Li-Cor, Lincoln, NE). *Amaranthus palmeri* plants were stored separately in paper bags and oven-dried at 65 C for 7 d to obtain dry biomass.

Statistical Analysis

TSW, ET_a, growth index, plant biomass, and total leaf area (TLA) responses were averaged over all subsampled replicates across study years. Data responses were averaged across study years, because crop type and *A. palmeri* combinations were not randomized across subplots. Thus, *A. palmeri* plants within each crop subplot were not independent replications. When data were averaged across study years, the crop subplots with and without *A. palmeri* were the experimental units for TSW and ET_a data analyses, while sampling date was the experimental unit for growth index, plant biomass, and TLA data analyses.

Table 2. Early-, mid-, and late-season date ranges within each time interval in 2019 and 2020.

Time interval	2019	2020
Early season	June 7–July 13	June 24–July 24
Midseason	July 19–September 2	August 2– August 28
Late season	September 8–October 4	September 5–September 29

Response analyses were run in PROC GLIMMIX within SAS v. 9.4 (SAS Institute, Cary, NC). TSW and ET_a responses were assumed to be normally distributed based on the residual plots. Variables included in the model were irrigation, crop type, presence of *A. palmeri*, and time of season in which the treatment response was measured. The time of season variable was created by separating dates across study years into early-, mid-, and late-season time intervals (Table 2). Within each time interval, five and four individual dates were included in 2019 and 2020, respectively. Individual dates were used as the level of replication for each of the irrigation, crop type, *A. palmeri*, and time of season variable combinations. Random effects included in the model accounted for whole-plot variation within a year between experimental units where irrigation was assigned; for split-plot variation due to the relationship between subplots; for variation between the time of season data that were measured within subplots throughout the experiment; and to fit a covariance structure to the residual variability that arose from the relationship between individual date measurements taken on the same experimental units within combinations of year, irrigation, crop type, and time of season. AR(1) and ARH(1) structures were utilized for the TSW and ET_a responses, respectively. Least-squares means (LSM) analyses were performed on means of each main effect (i.e., irrigation, crop type, presence of *A. palmeri*, and time of season) across years. A *t*-test was performed for all LSM analyses to indicate differences among the estimated means of the main effects.

Growth index, plant biomass, and TLA subsampled averages were skewed, with late-season responses having much larger values than early- and mid-season treatment responses. Based on the skewness and the fact that these treatment responses can only have values greater than zero, the responses were analyzed using a gamma distribution with a log link function (Lawless 2002; Nelson 1982). Final analyses for growth index, plant biomass, and TLA contained 48 observations, including data across 2 yr, two types of irrigation, three crop types, and four sampling dates. Averaging over the subsamples, year measurements were used as the level of replication; thus, variables included in the final model were irrigation, crop type, and sampling date. The model contained random effects accounting for whole-plot variation within a year between experimental units where irrigation was assigned and for split-plot variation due to the relationship between subplots.

Results and Discussion

TSW

Regarding the time of season effect, early-season TSW was greatest (308 mm), followed by similar midseason (288 mm) and late-season (290 mm) subsampled TSW means (Figure 2B). Neither irrigation method nor presence of 1 *A. palmeri* plant m^{-2} significantly affected TSW at the subplot level. Although 1 *A. palmeri* plant m^{-2} did not significantly affect mean subplot TSW in this study, it is plausible that *A. palmeri* density > 1 plant m^{-2} will have variable effects on

TSW given differing environmental conditions (Nielsen et al. 2016; Robinson and Nielson 2015; Unger and Vigil 1998). Studies conducted by Berger et al. (2015) and Massinga et al. (2003) found that crop fields with 1 *A. palmeri* plant m^{-2} have lower TSW than weed-free cropping systems. Several factors could have affected these results, including hard to control weeds that impacted subplot water use data (e.g., spotted spurge [*Chamaesyce maculata* (L.) Small]), low sample size for each treatment, and deeper rooting systems of *A. palmeri* compared with maize and soybean. Although root length and distribution of *A. palmeri* plants were not collected, the rooting system of *A. palmeri* plants likely extended beyond the depth of the soil-moisture sensors in the study (Wright et al. 1999), increasing the TSW around soil-moisture sensors in fallow subplots with *A. palmeri*.

According to a type III test of fixed effects for variable interactions and main effects, TSW was affected by crop type (P = 0.002) and time of season (P = 0.0023) across 2019 and 2020. Mean TSW was greatest in fallow subplots with and without *A. palmeri* (325 mm), followed by mean TSW in soybean subplots (291 mm) and maize subplots (269 mm) with and without *A. palmeri* (Figure 3A). These results were expected, as *A. palmeri* was the only plant extracting soil water in fallow subplots, while both *A. palmeri* and crops were extracting soil water in the maize and soybean subplots. These results are also supported by the fact that *A. palmeri* typically has a deeper root system than maize or soybean (Wright et al. 1999), allowing *A. palmeri* to extract soil water far below the soil-moisture sensors, resulting in higher mean TSW in fallow subplots.

Scaled Actual Evapotranspiration

According to a type III test of fixed effects for variable interactions and main effects, ET_a was affected by crop type and time of season interaction (P = 0.013) and by the presence of *A. palmeri* (P = 0.045) across 2019 and 2020. According to the simple effect comparisons of the crop type and time of season interaction, subplots with maize and soybean recorded statistically greater early-season ET_a of 28 to 30 mm and late-season ET_a of 7 to 8 mm compared with fallow subplots. Midseason subplot ET_a values in maize and soybean were similar, while fallow subplot ET_a was similar to maize and slightly lower than soybean subplot ET_a (Figure 3). Sugita et al. (2017) reported similar time of season changes of ET_a, where strong ET_a responses to irrigation or rain events occurred during earlier growth stages, and more stable ET_a responses occurred at the vegetative peak of the growing season. This is important, because *A. palmeri* can germinate and grow throughout an entire growing season (May to September) (Keeley et al. 1987). Although germinating late in the growing season may be detrimental to *A. palmeri* growth and seed production, optimal temperatures late into the growing season allow for rapid growth of *A. palmeri* while maize and soybean growth is beginning to slow, increasing the competitive ability of *A. palmeri* for water and nutrients that the crop also needs for seed production.

Regarding the presence of *A. palmeri* on ET_a, subplots with *A. palmeri* had greater ET_a of 28 mm compared with 23 mm in subplots without *A. palmeri* (Figure 4). Greater ET_a from subplots with *A. palmeri* can be attributed to the variable relationship between VWC and ET_a throughout the growing season (Wilson et al. 2020). In early spring, when V2-V3 crops and 18- to 25-cm *A. palmeri* were the primary sources of evapotranspiration, ET_a was strongly correlated with VWC. As crop and *A. palmeri* growth progressed, ET_a was largely independent of VWC as plants began to access water beyond the depth of the soil-moisture sensors. As the

(a)

(b)
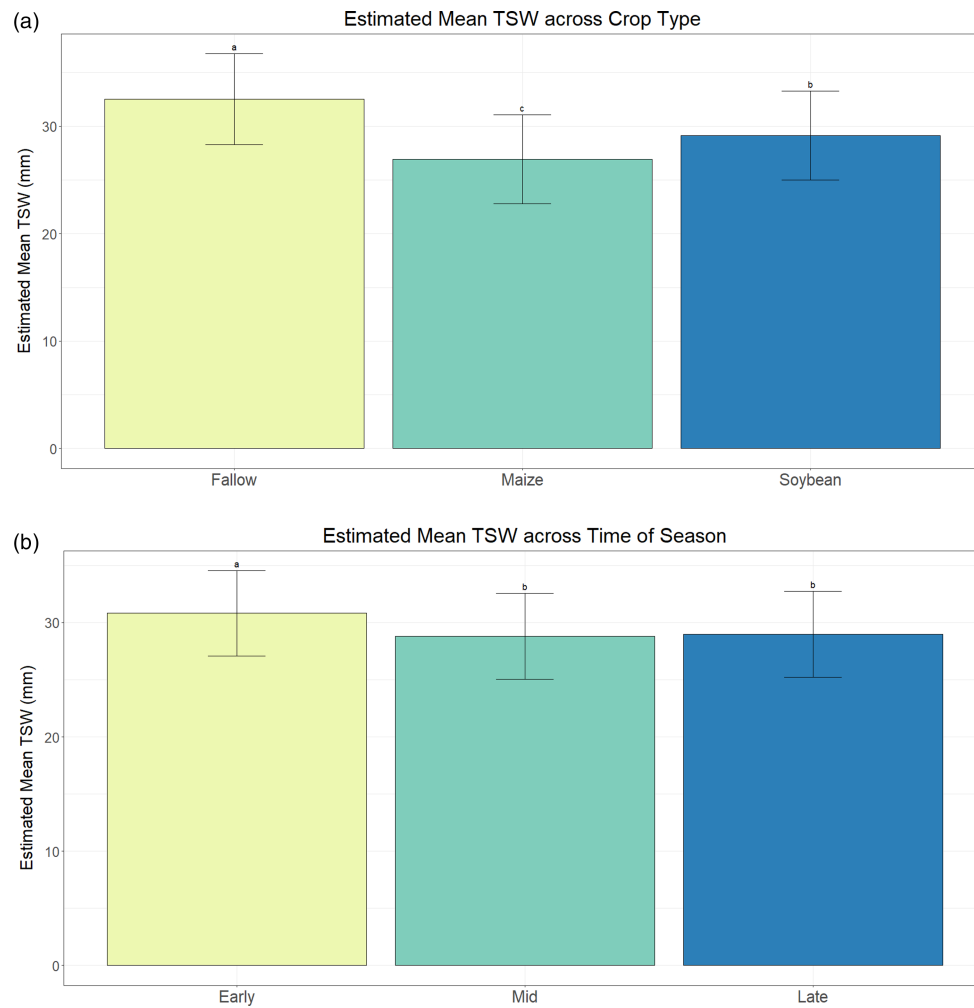
Figure 2. Estimated average total soil water (TSW, mm) across (A) crop type and (B) time of season in a study to determine evapotranspiration of *Amaranthus palmeri* in maize, soybean, and fallow under center-pivot and subsurface drip irrigation systems at the experimental site (University of Nebraska–Lincoln, South Central Agricultural Laboratory near Clay Center, NE). Standard error bars represent a 95% confidence interval. Different letters indicate significant differences between crop type and time of season (P ≤ 0.05).
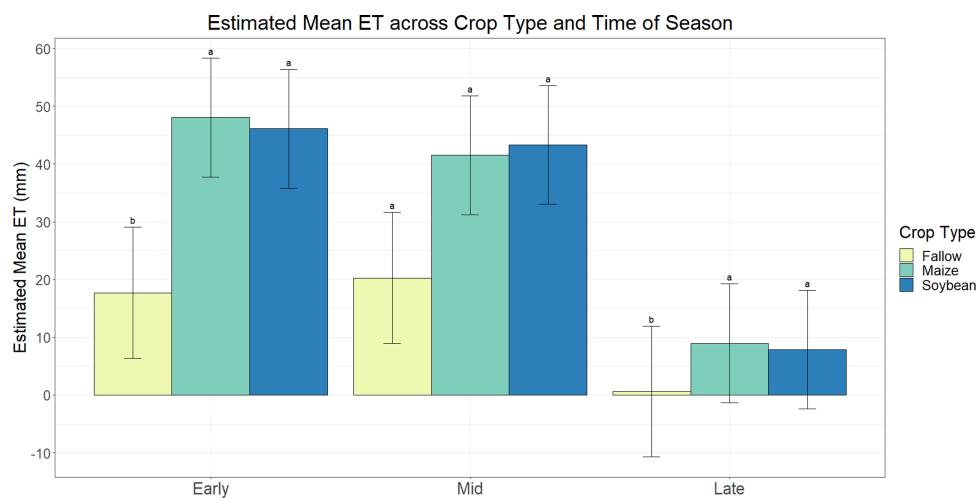
Figure 3. Estimated average actual evapotranspiration (ET, mm) across crop type and time of season in a study to determine evapotranspiration of *Amaranthus palmeri* in maize, soybean, and fallow under center-pivot and subsurface drip irrigation systems at the experimental site (University of Nebraska–Lincoln, South Central Agricultural Laboratory near Clay Center, NE). Standard error bars represent a 95% confidence interval. Different letters indicate significant differences between crop type and time of season (P ≤ 0.05).

Estimated Mean ET across Weed Species Levels
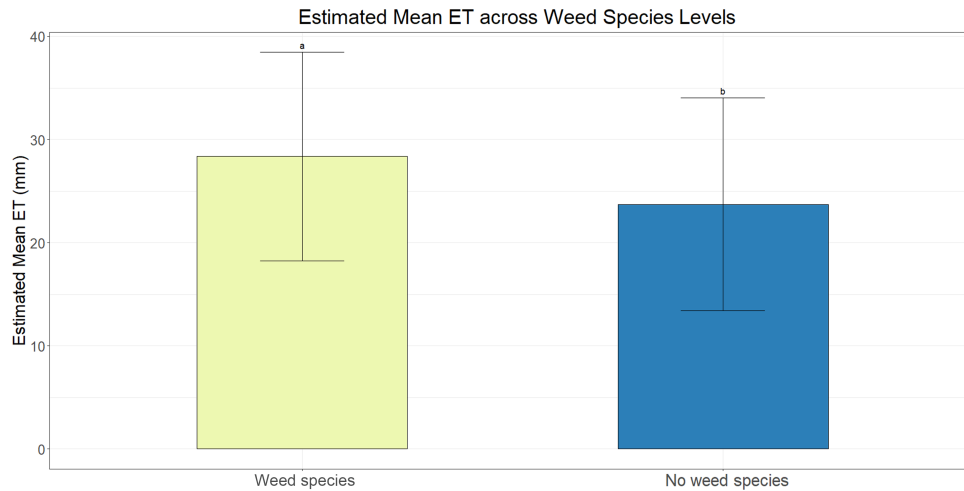
Figure 4. Estimated average actual evapotranspiration (ET, mm) of subplots with and without *Amaranthus palmeri* in a study to determine evapotranspiration of *Amaranthus palmeri* in maize, soybean, and fallow under center-pivot and subsurface drip irrigation systems at the experimental site (University of Nebraska–Lincoln, South Central Agricultural Laboratory near Clay Center, NE). Standard error bars represent a 95% confidence interval. Different letters indicate significant differences between subplots with and without *A. palmeri* ($P \leq 0.05$).
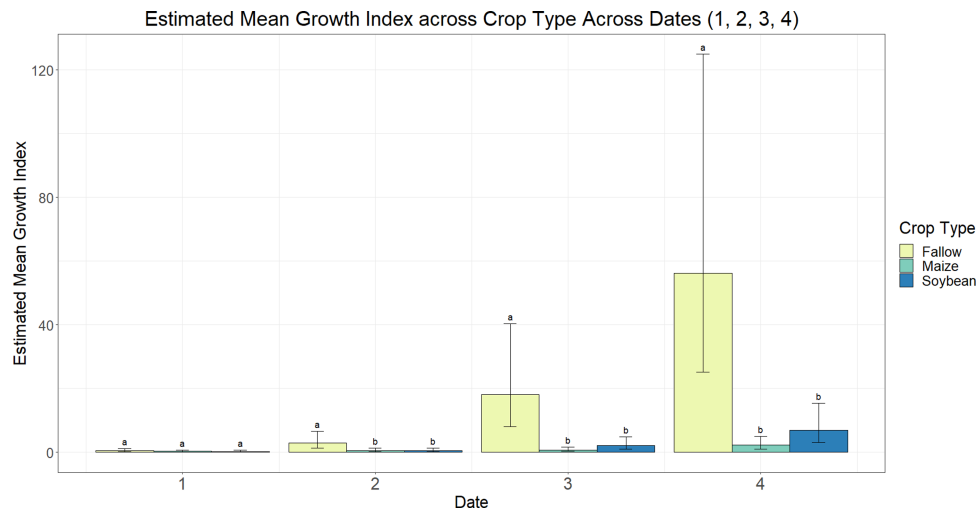
Figure 5. Estimated average of scaled *Amaranthus palmeri* growth index across crop type within each sampling date in a study to determine evapotranspiration of *Amaranthus palmeri* in maize, soybean, and fallow under center-pivot and subsurface drip irrigation systems at the experimental site (University of Nebraska–Lincoln, South Central Agricultural Laboratory near Clay Center, NE). Standard error bars represent a 95% confidence interval. Different letters indicate a significant difference between crop types within each sampling date ($P \leq 0.05$). Estimates are scaled down by a factor of 100,000 cm^3. Date 1: June 20, 2019, July 2, 2020; Date 2: July 2, 2019, July 14, 2020; Date 3: July 18, 2019, August 4, 2020; Date 4: August 8, 2019, August 26, 2020.

soil profile dried during the growing season, the correlation between ET_a and VWC emerged once again as the crop became largely dependent on irrigation. *Amaranthus palmeri* likely affected overall subplot ET_a, because the root system remained below 0.90 m and was less dependent on irrigation compared with the crops. Root length and root distribution of *A. palmeri* plants were not analyzed in this study, although these plant characteristics likely contributed to the ET_a differences seen in subplots with and without *A. palmeri* (Wright et al. 1999).

Growth Index, Plant Biomass, and TLA

According to a type III test of fixed effects for variable interactions and main effects, the mean growth index and mean biomass of *A. palmeri* were affected by a sampling date and crop type interaction across both study years ($P < 0.0001$). As expected, from the second

sampling date onward, the growth index and biomass of *A. palmeri* in fallow subplots were higher (0.3 to 5.6 m^3 and 0.06 to 1.27 kg, respectively) compared with *A. palmeri* in maize (0.06 to 0.23 m^3 and 0.008 to 0.03 kg, respectively) and soybean (0.06 to 0.7 m^3 and 0.01 to 0.16 kg, respectively) subplots (Figures 5 and 6). While *A. palmeri* growth index rates in maize and soybean were similar throughout the growing season, *A. palmeri* biomass was higher in soybean (0.05 to 0.16 kg) compared with maize (0.01 to 0.03 kg) at the third and fourth sampling dates (Figure 6). Mahoney et al. (2021) reported similar results, wherein taller weeds like *A. palmeri* were more competitive in fields with shorter crop canopies (e.g., soybean) and less competitive in crops that provide shading earlier in the growing season (e.g., maize), resulting in greater *A. palmeri* biomass in soybean systems (0.035 kg plant^{-1}) compared with maize systems (0.002 kg plant^{-1}). The reason for this is that when growing in competition with maize, *A. palmeri* allocates most of its resources
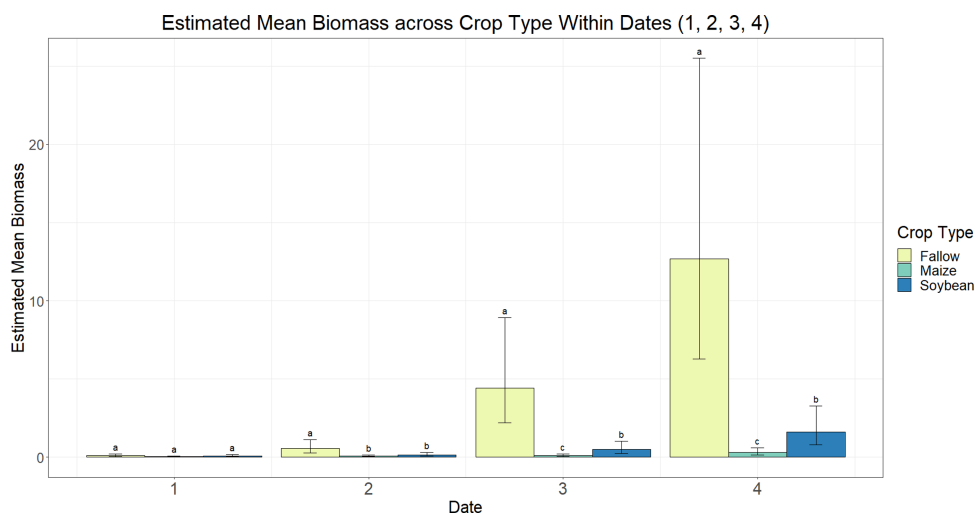
Figure 6. Estimated average of scaled *Amaranthus palmeri* biomass across crop type within each sampling date in a study to determine evapotranspiration of *Amaranthus palmeri* in maize, soybean, and fallow under center-pivot and subsurface drip irrigation systems at the experimental site (University of Nebraska–Lincoln, South Central Agricultural Laboratory near Clay Center, NE). Standard error bars represent a 95% confidence interval. Different letters indicate a significant difference between crop types within each sampling date (P ≤ 0.05). Estimates are scaled down by a factor of 100 g. Date 1: June 20, 2019, July 2, 2020; Date 2: July 2, 2019, July 14, 2020; Date 3: July 18, 2019, August 4, 2020; Date 4: August 8, 2019, August 26, 2020.

toward vertical growth, whereas in competition with soybean, *A. palmeri* first allocates most of its resources toward vertical growth. Once it reaches the soybean height, *A. palmeri* begins allocating most of its resources toward lateral growth, resulting in more branching and thus greater biomass production. These results are not surprising, given *A. palmeri*'s rapid growth rate (Culpepper et al. 2010; Horak and Loughin 2000), biomass accumulation (Sellers et al. 2017), and photosynthetic rate three to four times that of maize, soybean, and cotton (*Gossypium hirsutum* L.) (Steckel 2007).

According to a type III test of fixed effects for variable interactions and main effects, *A. palmeri* TLA was affected by a sampling date, irrigation, and crop type interaction across both years (P = 0.023). Similar to *A. palmeri* growth index and biomass results, differences in *A. palmeri* TLA across crop type were evident from the second sampling date until the end of the growing season. The TLA of *A. palmeri* in fallow subplots was greater (41 to 2,575 m^2) compared with maize (6.6 to 17.8 m^2) and soybean (10.0 to 47.6 m^2) subplots, which correlates with *A. palmeri* growth index and biomass results. An irrigation effect on TLA was detected, although this is likely due to the missing TLA data points of *A. palmeri* in fallow subplots under CPI and SDI in 2020. Due to a severe hailstorm the evening before the sampling date, only one *A. palmeri* in the fallow subplot under CPI was sampled for TLA in 2020, resulting in skewed *A. palmeri* TLA under SDI from an outlier in 2019. Thus, sampling date and crop type are the variables more likely to affect TLA in this study.

Practical Implications

This is the first study evaluating the actual evapotranspiration (ET_a) of *A. palmeri* in multiple crops under CPI and SDI with the goal of finding an irrigation effect on *A. palmeri* ET_a. The results indicate differences in *A. palmeri* ET_a between time of season (early, mid-, and late season) and crop species across 2019 and 2020. While our analyses indicate irrigation contributes to differences in mid- and late-season *A. palmeri* TLA between crop species, irrigation did not affect subplot or sub-subplot ET_a, TSW, or *A. palmeri* growth index or biomass. Additionally, the irrigation

effect on *A. palmeri* TLA is likely a result of missing TLA data at the fourth sampling date in 2020.

Although irrigation did not significantly affect subplot data, the presence of *A. palmeri* did have an impact on sub-subplot ET_a across both years. This can be attributed to the variable relationship between VWC and ET_a throughout the growing season due to advancing phenological stages and management practices. As crop and *A. palmeri* growth progressed, ET_a was largely independent of VWC as plants began to access water beyond the depth of the soil-moisture sensors. As the soil profile dried during the growing season, the correlation between ET_a and VWC emerged once again as the crop became largely dependent on irrigation. However, *A. palmeri* likely affected overall sub-subplot ET_a, because the root system remained below 0.90 m and was less dependent on irrigation compared with the crops. Root length and root distribution of *A. palmeri* plants were not analyzed in this study, although these data parameters likely contributed to the ET_a differences seen in subplots with and without *A. palmeri*. Thus, future studies exploring weed species' water use should measure root length and root distribution using soil-moisture sensors over the entire rooting profile of the plant to better understand the relationship between VWC and ET_a. As indicated by the time of season effect on TSW and ET_a, irrigation or rain events, along with plant phenotypical development, can significantly influence the TSW and ET_a relationship. These observations hold significance for growers who are considering irrigation expansion and upgradation. Selecting an SDI system may lower water use due to reduced evaporation; however, the presence of a heavy *A. palmeri* infestation in an SDI field may increase competition for water between *A. palmeri* and the crop, because the irrigated water is more readily available to plants. The rooting depth and distribution of *A. palmeri* under differing irrigation systems will need to be quantified and compared with water use data to make an accurate assessment of irrigation choice.

Traditionally, crop system suitability, irrigation efficiency, and investment cost are factors that determine selection among CPI and SDI systems. However, results of this study suggest that weed–crop competition should also be considered, making irrigation

method selection a holistic process that weighs both biotic and abiotic consequences. This study provides fundamentally critical information on *A. palmeri* evapotranspiration and its relation to *A. palmeri* morphological features (e.g., growth index, biomass, and TLA) for future use in mechanistic (and empirical) weed–crop competition models. ET_a is highly location specific and is driven by weather, soils, and farm management; thus, further research on ET_a of economically important broadleaf and grass weed species should be conducted under diverse environments to build a robust database.

Other economically important weed species such as velvetleaf (*Abutilon theophrasti* Medik.), common lambsquarters (*Chenopodium album* L.), and giant foxtail (*Setaria faberi* Herrm.) in row-crop production would likely result in lower ET_a due to lower competitive phenotypes compared with *A. palmeri*. Root depth and distribution, along with growth rate, are factors that would need to be considered when comparing water use of multiple weed species and the effect of varying irrigation methods on water use. The ET_a results for *A. palmeri* would likely differ in other environments as well, demonstrating the need for more research of this nature conducted in diverse environments. Ehleringer (1983) reported the net rate of *A. palmeri* photosynthesis is temperature dependent, with the optimum range occurring between 36 C and 46 C. The average daytime temperatures in July and August in south-central Nebraska are 29 C and 30 C, respectively (NCEI 2020). If this same study were conducted in the southern United States, *A. palmeri* plants would likely have higher rates of ET_a because of higher rates of photosynthesis due to higher average temperatures, likely increasing *A. palmeri* growth index, biomass, and TLA. To effectively build a robust database of the interaction of evapotranspiration (i.e., water use) and morphological features of economically important agronomic weed species, this type of research should be implemented across various and diverse environments.

References

Appleby AP, Muller F, Carpy S (2000) Weed control. Pages 687–707 *in* Muller F, ed. Agrochemicals. New York: Wiley

Berger ST, Ferrell JA, Rowland DL, Webster TM (2015) Palmer amaranth (*Amaranthus palmeri*) competition for water in cotton. Weed Sci 63:928–935

Bryant KJ, Benson VW, Kiniry JR, Williams JR, Lacewell RD (1992) Simulating corn yield response to irrigation timings: validation of the EPIC model. J Prod Agric 5:237–242

Chahal PS, Irmak S, Jugulam M, Jhala AJ (2018) Evaluating effect of degree of water stress on growth and fecundity of Palmer amaranth (*Amaranthus palmeri*) using soil moisture sensors. Weed Sci 66:738–745

Chauhan BS, Johnson DE (2010) The role of seed ecology in improving weed management strategies in the tropics. Adv Agron 105:221–262

Cousens R, Brain P, O'Donovan JT, O'Sullivan PA (1987) The use of biologically realistic equations to describe the effects of weed density and relative time of emergence on crop yield. Weed Sci 35:720–725

Culpepper AS, Webster TM, Sosnoskie LM, York AC (2010) Glyphosate-resistant Palmer amaranth in the US. Pages 195–212 *in* Nandula VK, ed. Glyphosate Resistance in Crops and Weeds. Hoboken, NJ: Wiley

De Sanctis JH, Jhala AJ (2021) Interaction of dicamba, fluthiacet-methyl, and/or glyphosate for control of velvetleaf in dicamba/glyphosate-resistant soybean. Weed Technol 35:761–767

Diggle AJ, Neve PB, Smith FP (2003) Herbicides used in combination can reduce the probability of herbicide resistance in finite weed populations. Weed Res 43:371–382

Djaman K, Irmak S (2012) Soil water extraction patterns and crop-, irrigation-, and evapotranspiration water use efficiency of maize under full and limited irrigation and rainfed settings. Trans ASABE 55:1223–1238

Ehleringer J (1983) Ecophysiology of *Amaranthus palmeri*, a Sonoran Desert summer annual. Oecologia 57:107–112

Ehleringer J (1985) Annuals and perennials of warm deserts. Page 162–180 *in* Chabot BF, Mooney HA, eds. Physiological Ecology of North American Plant Communities. Dordrecht, Netherlands: Springer

Ehleringer J, Forseth I (1980) Solar tracking by plants. Science 210:1094–1098

Firbank LG, Watkinson AR (1985) A model of interference within plant monocultures. J Theor Biol 116:291–311

Franssen AS, Skinner DZ, Al-Khatib K, Horak MJ, Kulakow PA (2001) Interspecific hybridization and gene flow of ALS resistance in *Amaranthus* species. Weed Sci 49:598–606

Heap I (2014) Herbicide resistant weeds. Pages 281–301 *in* Pimentel D, Peshin R, eds. Integrated Pest Management. Dordrecht, Netherlands: Springer

Horak MJ, Loughin TM (2000) Growth analysis of four *Amaranthus* species. Weed Sci 48:347–355

Irmak S (2010) Nebraska water and energy flux measurement, modeling, and research network (NEBFLUX). Trans ASABE 53:1097–1115

Irmak S (2015) Inter-annual variation in long-term center pivot-irrigated maize evapotranspiration (ET) and various water productivity response indices: Part I. Grain yield, actual and basal ET, irrigation-yield production functions, ET-yield production functions, and yield response factors. J Irrig Drain Eng 141:1–17.

Irmak S (2019a) Perspectives and Considerations for Soil Moisture Sensing Technologies and Soil Water Content- and Soil Matric Potential-based Irrigation Trigger Values. Lincoln: Extension NebGuide 3045. 8 p

Irmak S (2019b) Soil-Water Potential and Soil-Water Content Concepts and Measurement Methods. Lincoln, NE: Extension Circular EC3046. 18 p

Irmak S, Burgert MJ, Yang H, Cassman KG, Walters DT, Rathje WR, Payero JO, Grassini P, Kuzila MS, Brunkhorst KJ, Eisenhauer DE, Kranz WL, VanDeWalle B, Rees JM, Zoubek GL, et al. (2012) Large scale on-farm implementation of soil moisture-based irrigation management strategies for increasing maize water productivity. Trans ASABE 55:881–894

Irmak S, Haman DZ, Irmak A, Jones JW, Campbell KL, Crisman TL (2004) Measurement and analysis of growth and stress parameters of *Viburnum odoratissimum* (Ker-gawl) grown in a multi-plot box system. HortScience 39:1445–1455

Irmak S, Payero J, VanDeWalle B, Rees J, Zoubek G, Martin D, Kranz W, Eisenhauer D, Leininger D (2016) Principles and Operational Characteristics of Watermark Granular Matrix Sensor to Measure Soil Water Status and Its Practical Applications for Irrigation Management in Various Soil Textures. Lincoln, NE; Extension Circular EC783. 14 p

Keeley PE, Carter CH, Thullen RJ (1987) Influence of planting date on growth of Palmer amaranth (*Amaranthus palmeri*). Weed Sci 35:199–204

Lawless JF (2002) Statistical Models and Methods for Lifetime Data. 2nd ed. Hoboken, NJ: Wiley. Pp 25, 164–170

Mahoney DJ, Jordan DL, Hare AT, Leon RG, Roma-Burgos N, Vann MC, Jennings KM, Everman WJ, Cahoon CW (2021) Palmer amaranth (*Amaranthus palmeri*) growth and seed production when in competition with peanut and other crops in North Carolina. Agron J 11:1734

Massinga RA, Currie RS, Trooien TP (2003) Water use and light interception under Palmer amaranth (*Amaranthus palmeri*) and corn competition. Weed Sci 51:523–531

Mohler CL (2004) Enhancing the competitive ability of crops. Pages 269–321 *in* Liebman M, Mohler CL, Staver CP, eds. Ecological Management of Agricultural Weeds. Cambridge: Cambridge University Press

Monteith JL (1965) The state of movement of water in living organisms: evaporation and environment. Pages 205–234 *in* Proceedings of the Society of Experimental Biology, Symposium 19. Cambridge: Cambridge University Press

Nelson W (1982) Applied Life Data Analysis. 1st ed. Hoboken, NJ: Wiley. Pp 44–47

Neve P, Diggle AJ, Smith FP (2003) Simulating evolution of glyphosate resistance in *Lolium rigidum* I: population biology of a rare resistance trait. Weed Res 43:404–417

Nielsen DC, Lyon DJ, Higgins RK, Hergert GW, Holman JD, Vigil MF (2016) Cover crop effect on subsequent wheat yield in the central Great Plains. Agron J 108:243–256

[NCEI] NOAA National Centers for Environmental Information (2020) Climate Normals. https://www.ncei.noaa.gov/products/land-based-station/us-climate-normals. Accessed: August 31, 2023

Pantone DJ, Baker JB (1991) Reciprocal yield analysis of red rice (*Oryza sativa*) competition in cultivated rice. Weed Sci 39:42–47

Paredes P, Rodrigues GC, Alves I, Pereira LS (2014) Partitioning evapotranspiration, yield prediction and economic returns of maize under various irrigation management strategies. Agric Water Manag 135:27–39

Park SE, Benjamin LR, Watkinson AR (2002) Comparing biological productivity in cropping systems: a competition approach. J Appl Ecol 39:416–426

Peltzer S, Dougla A, Diggle AJ, George W, Renton M (2012) The Weed Seed Wizard: have we got a solution for you! Pages 99–102 *in* Proceedings of the 18th Australasian Weeds Conference. Victoria, Melbourne: Weed Society of Victoria

Robinson C, Nielsen D (2015) The water conundrum of planting cover crops in the Great Plains: when is an inch not an inch? Crops Soils 48:24–31

Sarangi D, Irmak S, Lindquist JL, Knezevic SZ, Jhala AJ (2015) Effect of water stress on the growth and fecundity of common waterhemp (*Amaranthus rudis*). Weed Sci 64:42–52

Sellers BA, Smeda RJ, Johnson WG, Kendig JA, Ellersieck MR (2017) Comparative growth of six *Amaranthus* species in Missouri. Weed Sci 51:329–333

Singh M, Kaur S, Chauhan BS (2020) Weed interference models. Pages 117–142 *in* Chantre G, Gonzalez-Andujar J, eds. Decision Support Systems for Weed Management. Cham, Switzerland: Springer

Steckel LE (2007) The dioecious *Amaranthus* spp.: here to stay. Weed Technol 21:567–570

Sugita M, Matsuno A, El-Kilani RM, Abdel-Fattah A, Mahmoud MA (2017) Crop evapotranspiration in the Nile delta under different irrigation methods. Hydrolog Sci J 62:1618–1635

Unger PW, Vigil MF (1998) Cover crop effects on soil water relationships. J Soil Water Conserv 53:200–207

Van Acker RC (2009) Weed biology serves practical weed management. Weed Res 49:1–5

Wilson TG, Kustas WP, Alfieri JG, Anderson MC, Gao F, Prueger JH, McKee LG, Alsina MM, Sanchez LA, Alstad KP (2020) Relationship between soil water content, evapotranspiration, and irrigation measurements in a California drip-irrigated Pinot noir vineyard. Agric Water Manag 237, 10.1016/j.agwat.2020.106186

Wright SR, Jennette MW, Coble HD, Rufty TW Jr (1999) Root morphology of young *Glycine max*, *Senna obtusifolia*, and *Amaranthus palmeri*. Weed Sci 47:706–711